ACS Chemical Neuroscience

Research Article

pubs.acs.org/chemneuro

Delivery and Tracking of Quantum Dot Peptide Bioconjugates in an Intact Developing Avian Brain

Rishabh Agarwal,[†] Miriam S. Domowicz,[‡] Nancy B. Schwartz,[‡] Judy Henry,[‡] Igor Medintz,[§] James B. Delehanty,[§] Michael H. Stewart,[∥] Kimihiro Susumu,[∥] Alan L. Huston,[∥] Jeffrey R. Deschamps,[§] Philip E. Dawson,[⊥] Valle Palomo,[⊥] and Glyn Dawson*[,†,#]

[†]Committee on Neurobiology and [‡]Department of Pediatrics, University of Chicago, Chicago, Illinois 60637, United States

[§]Center for Bio/Molecular Science and Engineering, Code 6900, and [∥]Optical Sciences Division, Code 5611, U.S. Naval Research Laboratory, Washington, DC 20375, United States

[⊥]Scripps Research Institute, La Jolla, California 92037, United States

[#]Departments of Pediatrics, Biochemistry and Molecular Biology, University of Chicago, Chicago, Illinois 60637, United States

ABSTRACT: Luminescent semiconductor ~9.5 nm nanoparticles (quantum dots: QDs) have intrinsic physiochemical and optical properties which enable us to begin to understand the mechanisms of nanoparticle mediated chemical/drug delivery. Here, we demonstrate the ability of CdSe/ZnS core/shell QDs surface functionalized with a zwitterionic compact ligand to deliver a cell-penetrating lipopeptide to the developing chick embryo brain without any apparent toxicity. Functionalized QDs were conjugated to the palmitoylated peptide WGDap-(Palmitoyl)VKIKKP9GGH6, previously shown to uniquely facilitate endosomal escape, and microinjected into the embryonic chick spinal cord canal at embryo day 4 (E4). We were subsequently able to follow the labeling of spinal cord extension into the ventricles, migratory neuroblasts, maturing brain cells, and complex structures such as the choroid plexus. QD intensity extended throughout the brain, and peaked between E8 and E11 when fluorescence was concentrated in the choroid plexus before declining to hatching (E21/P0). We observed no abnormalities in embryonic patterning or embryo survival, and mRNA in situ hybridization confirmed that, at key developmental stages, the expression pattern of genes associated with different brain cell types (brain lipid binding protein, Sox-2, proteolipid protein and Class III-β-Tubulin) all showed a normal labeling pattern and intensity. Our findings suggest that we can use chemically modified QDs to identify and track neural stem cells as they migrate, that the choroid plexus clears these injected QDs/nanoparticles from the brain after E15, and that they can deliver drugs and peptides to the developing brain.

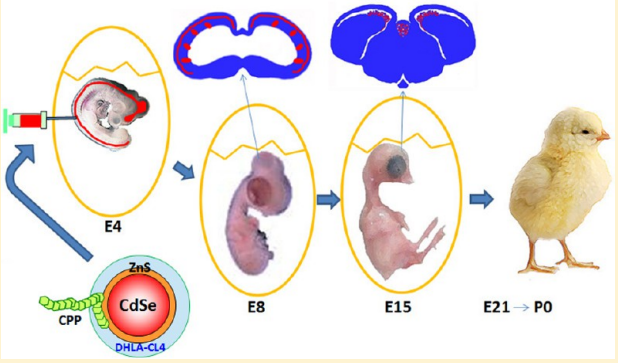

KEYWORDS: *Nanoparticles, zwitterion, quantum dots, peptidyl delivery, normal embryonic chick brain development, choroid plexus*

A major obstacle to the treatment of neurological diseases with small molecules or peptides/proteins is the delivery to individual cells in the central nervous system. For small molecules, the overall charge of the molecule and a mechanism to prevent sequestration in the endosome are thought to be critical factors. For example, positively charged dopamine does not cross the blood-brain barrier, whereas its zwitterionic precursor (3,4-dihydroxyphenylalanine or L-DOPA) readily crosses the barrier and is taken up by neurons to relieve some of the symptoms of Parkinson's disease.[1] For larger peptides or proteins, a specific targeting sequence has been employed with limited success, for example, the 29 amino acid RVG sequence from the rabies surface coat protein[2,3] or a synthetic peptide based on the positively charged TAT peptide.[4,5] As an initial step toward designing a vehicle that could deliver biologically active chemicals into the brain, we previously showed that JB577, a pharmacological chaperone (an inhibitor of palmitoyl:protein thioesterase based on palmitoylated-K-Ras4A C-terminal sequence required for membrane association) could uniquely promote both membrane penetration and endosomal escape.[6,7] This chaperone lipopeptide contained a positively charged lysine-rich region and a noncleavable palmitic acid tail. We then appended the peptide tail with a polyproline sequence and a glycine spacer together with a 6 amino acid polyhistidine domain which allowed it to self-assemble by binding to Zn on the surface of luminescent CdSe/ZnS semiconductor quantum dots (QDs). The intense QD fluorescent signal along with peptide presentation in a localized high avidity format allowed us to evaluate peptide functional properties in a variety of cell lines and a hippocampal brain slice

Received: January 14, 2015
Revised: February 10, 2015
Published: February 17, 2015

DOI: 10.1021/acschemneuro.5b00022
ACS Chem. Neurosci. 2015, 6, 494−504

model.[6,8,9] A series of Förster resonance energy transfer studies confirmed that the peptide stayed associated with the QD for at least 72 h, and this study confirms that QDs coated with specific types of chemical coatings are stable nanoparticles that can be utilized to understand many of the mechanistic processes and intricacies surrounding the burgeoning field of nanoparticle-mediated drug delivery both in vitro and in vivo.[10]

QDs have the advantage that they can be inherently chemically synthesized with a discrete and narrow emission profile by adjusting their physical dimensions, and their spectral properties allow them to fluoresce intensely and with extended longevity.[7,9,11] Furthermore, the surface physiochemical properties and character of the QD can be engineered to specifically target a particular type of cell or tissue. It has been previously shown that coating the QDs with negatively charged carboxyl groups increased leukocyte adherence and migration whereas positively charged amino groups and neutral PEG did not.[12] Other studies have focused on further modification of the QD surface with active targeting moieties, for example, an RGD sequence ligand specifically targeted QDs to brain tumors,[13] whereas an in vivo injection of uncoated (neutral) QDs into the hippocampus of live mice mainly targeted the QDs to microglia.[14] These and other similar results confirm that the coating of QDs can affect its destination following injection. More importantly, multifunctional QDs have been demonstrated to deliver an active druglike cargo of siRNA to knockdown EGFRvIII receptors in human glioma cells,[15] suggesting that QDs can be designed to deliver cargo to a specified target cell type. However, there is still limited data reagarding their fate in an intact normal brain and no conclusive studies conducted on the fate of chemically modified QDs injected into a developing brain.

We have previously reported that CdSe/ZnS core/shell QDs coated with a dihydrolipoic acid (DHLA)-based zwitterionic compact ligand were able to specifically target QDs to neurons, with minimal uptake by glial cells or microglial cells, in actively myelinating and physiologically intact rat hippocampal slices.[9] The combination of small size (≤10 nm hard diameter), uniquely intense spectral properties, the ability to synthesize different compact zwitterionic ligand coatings, and the ability to spontaneously conjugate to JB577 peptide enabled us to follow their fate after injection into embryonic chick brain. We have achieved the successful introduction of such QDs by a novel microinjection procedure at an early embryonic stage of development and can demonstrate the extensive brain distribution in a developing central nervous system without overtly affecting brain development, despite the rapid increase in size and complexity of the brain during this period.

The developing chick embryonic brain presents numerous advantages for assessing the ability of QDs to deliver a chemical cargo such as JB577 (and/or other bioactive peptides) to all parts of a developing nervous system. While rats and mice have often been used to study embryonic neuronal and glial cell differentiation and migration,[16,17] this requires the use of timed pregnant mice, and large mouse colonies in order to get enough embryos. Furthermore, although methods for electroporation and viral infection have been established for both mouse and chick, the in ovo method is much simpler than the in utero method. The chick model also allows for larger sample sizes, ease of handling, and the ability to harvest brains at precise developmental intervals. The chick model is absent of confounding maternal or placental influences and upon hatching, has a comparable developmental maturity to the human brain by birth.[18] We chose to microinject the QDs at embryonic day 4 (E4), because at this age the chick brain consists of a neuroepithelium that differentiates in waves to eventually generate the neurons, astrocytes, and oligodendrocytes that form functional centers in a schedule consistent with that observed in mammals. The chick is therefore a model whose embryonic development is well-studied and documented, and the anatomy of the brain is well-defined in particular for the laminar structure of the optic tectum in the midbrain.[19,20] We have not previously observed any gross toxicity with the CdSe/ZnS QDs in cells or actively myelinating neonatal rat hippocampal slices,[9] and our experience with interventions in the developing chick embryo in vivo suggested that injecting the QDs at E4 would cause minimal trauma and injury to the embryo and not result in major experimental embryo death. We therefore utilized the chick as a system in which to follow the distribution of peptide-functionalized QDs to a developing brain without adversely affecting critical brain structures or their function.

RESULTS AND DISCUSSION

Synthesis of QD-Peptide Bioconjugates. We started with 625 nm emitting CdSe/ZnS core/shell QDs with a quantum yield in PBS of ∼50%. These bright red emitting QDs provided for easy distinction and separation of QD fluorescence from naturally occurring autofluorescence in the dense chicken embryonic brain tissue. We initially began testing delivery with QDs surface functionalized and made hydrophilic with DHLA derivatives displaying either a long, neutral PEG moiety or a far more compact zwitterionic functional group (CL4: see Figure 1 for ligand structures and schematics of the QD-peptide conjugates[21,22]). The PEG mediated colloidal stability across a broad pH range via its ∼15 ethylene oxide repeats, while the CL4 exploited its zwitterionic nature to accomplish the same goal while significantly reducing the QDs hydrodynamic size. Both ligands are also known for their nonfouling and nonbinding nature and were superior to a range of other coats tested.

The relatively large surface area of these ∼9.5 nm diameter 625 nm emitting QDs (266 ± 25 nm^2 with a radius of 4.6± 0.4 nm) provided for the optimal conjugation of a 25:1 ratio of peptide:QD or as required.[8,23] For the controlled display of peptides on the QD surface, we relied on the metal affinity driven coordination of polyhistidine sequences, $(His)_n$, with the ZnS outer shell of the QD.[8−2126] This rapid, high-affinity cooperative interaction only required mixing of the requisite amounts of peptide per QD and in many cases provided for control over the ratio of peptide displayed per QD along with the subsequent orientation.[24] The peptide tested was a chemical chaperone (GDap[palmitoyl]VKIKK, based on the ras-4A palmitoylation site) designed to promote the refolding of misfolded protein (palmitoyl:protein thioesterase) when delivered to cells. This lipopeptide is part of the cell penetrating Palm-1 lipopeptide referred to here as JB577[8] and was chosen for its unique ability to effect both cellular delivery and endosomal escape of various nanoparticles in a nontoxic manner.[8] The modular nature of the peptide sequence, W•G•Dap(Palmitoyl)•VKIKK•P9•GG•H6 with a peptide bond "•" separating functional modules, provided several desired functions to the peptide. The final peptide includes Trp (W) for monitoring peptide purification via UV−vis absorption; Gly2 as flexible hinges and Dap(Palmitoyl) and VKIKK (based on the K-Ras4A C-terminal sequence utilized

DOI: 10.1021/acschemneuro.5b00022
ACS Chem. Neurosci. 2015, 6, 494−504

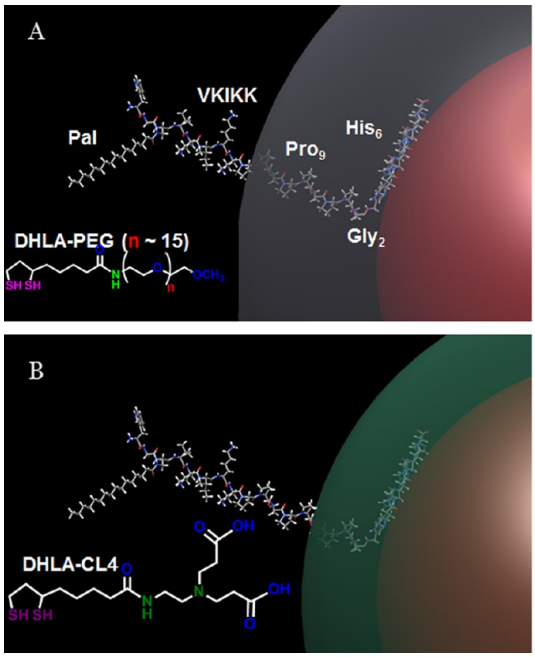

Figure 1. Schematic depicting the QD-peptide structure. (A) Schematic representation of 625 nm QDs surface functionalized with DHLA-PEG (QD-PEG-JB577) and displaying the palmitoylated peptide (JB577) assembled by polyhistidine linkage. The 625 nm QD (diameter ~10 nm) is shown in red, and the PEG as a gray shell extending 30 Å from the QD surface. The peptide is shown in a ball and stick structure appended onto the QD by the hexahistidine sequence. Functional residues along with the position of the palmitate (Pal) group are indicated as well. The Gly2-Pro9 portion of the peptide is shown as almost completely enveloped in the PEG layer. (B) Schematic representation of the 625 QD surface functionalized with DHLA-CL4 (green shell) and binding the same peptide (QD-CL4-JB577). The structures for each respective ligand are shown inset.

for membrane association and penetration) to jointly provide for endosomal release in a manner that is still not fully understood. $(Pro)_9$ acts as a rigid linker that displaces the peptide N-terminus away from the QD surface and prevents it from folding back on the QD (in the case of PEGylated ligands). The $(His)_6$ binds the Zn molecules on the QD surface and thereby mediates long-term peptide attachment to the QD[8]. Similar QDs have been reported to be stable in monkey brain for at least 90 days.[27]

Initial Comparison of PEG and CL4 Coated QDs. Given the challenging nature of the environment in which the QD-peptide conjugates would be placed, we initially sought to determine the optimal ligand coating for these experiments. Embryos at E4 were injected in the spinal cord canal with either CL4-coated or PEG-coated QDs assembled with a ratio of 25 JB577 per QD following the protocol described in the Methods. These embryos were then harvested and sectioned at embryonic stage E6. The distribution of both the CL4-coated and PEG-coated QDs were then visually analyzed in longitudinal sections (40 μm) from comparable regions along the spinal column (see Figure 2). Clusters of fluorescence appeared more frequently with PEG-QDs as compared to CL4-QDs although the reasons for this observation are not understood at the present time. One possibility is that the extended length of the PEG surface on the QD could result in the screening or obscuring of a key portion of the JB577 needed for cellular uptake or tissue binding in this particular context. The more compact CL4 surface allows such interactions to occur. Additionally zwitterionic groups are commonly found in biological systems and are one of the primary mechanisms by which proteins remain both soluble and noninterfering. The CL4-QD peptide conjugates were better tolerated in this environment.[25] Supporting this latter notion, Muro et al. reported that QDs coated with a structurally similar zwitterionic DHLA-sulfobetaine group remained far more dispersed and were far better tolerated in both HeLa cells and *Xenopus laevis* embryos than QDs capped with micelles or polymers.[26] Aggregation of QDs *in vivo* is believed to increase the risk of cell-toxicity.[27] Therefore, in terms of coupling and stability *in vivo* and minimizing any potential toxicity issues, the CL4-coated QDs were utilized throughout the rest of the study, and in conjunction with the JB577 peptide. These are referred to hereafter as "QD-CL4-JB577".

Evidence for Migratory Neuroblast Tracks. Using just the QD-CL4-JB577 conjugates, we continued on with our experimental format and observed clear and extensive clonal

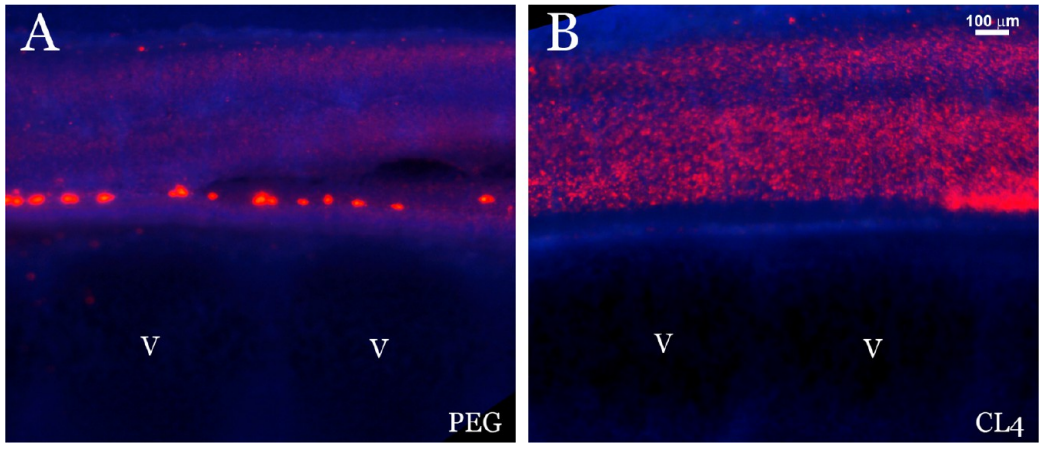

Figure 2. Comparison of the fate of QD-PEG-JB577 and QD-CL4-JB577 microinjected into in vivo embryos at E4. Representative sagittal 40 μm section through the spinal cord of E6 embryos injected at E4. (A) Injected with QD-PEG-JB577 peptide conjugate. (B) Injected with QD-CL4-JB577 peptide conjugate. QDs are red and DAPI stained nuclei are blue. A more uniform dispersion of the QDs with the CL4 coating is observed compared to PEG. The position of the vertebrae is indicated (V). The results presented here and in the following images are representative of 5 independent injection experiments each involving 18 control and 18 QD-injected embryos.

DOI: 10.1021/acschemneuro.5b00022
ACS Chem. Neurosci. 2015, 6, 494−504

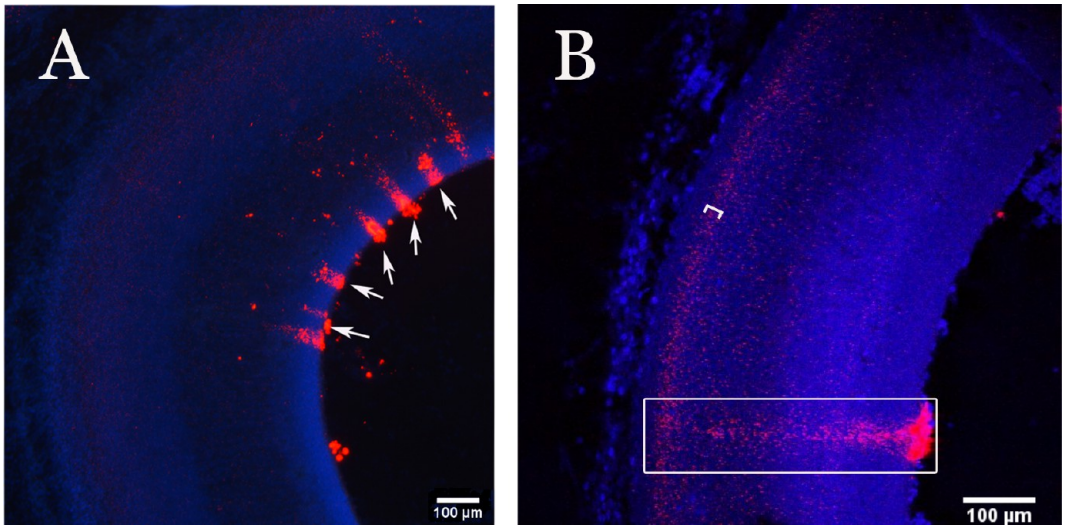

Figure 3. Uptake and migration of the QD-peptide conjugates. Coronal 40 μm sections through midbrain of embryos injected at E4 with QD-CL4-JB577 peptide conjugates (red) and collected at E8. (A) Uptake of QDs (red) from the ventricles and evidence of long distance migration (arrows) most likely along glial tracks. (B) Higher magnification picture showing a columnar distribution of dots (box) in neuroblast migratory tracks. Another layer of cells with heavier content of QDs is indicated with a bracket, further confirming their intracellular localization.

dispersion of the QDs, and the representative example provided in Figure 3 shows them visualized in the E8 midbrain. The QD-CL4-JB577 conjugates always appeared to be distributed along several parallel "tracks" extending radially outward from the ventricular zone. This distribution most likely indicates that several neural stem cells located in the ventricular surface[28] at the time of injection had taken up massive amounts of QDs and distributed them to their progeny. At the time of injection, E4, most of the neural stem cells are expected to express SOX2,[29,30] maintain a radial glial morphology, and generate neuroblasts.[31] Following this, during the subsequent 2 days, the newly generated neuroblasts should migrate radially to their specific layer location along the radial glial tracks in the midbrain.[31] Thus, the observed columnar distribution of cells at E8 (Figure 3) could represent neuroblasts migrating radially and carrying the QDs with them. Furthermore, a layer of heavily QD labeled cells can be distinguished which corresponds to the densely packed neuronal nuclei layer confirming their intracellular localization (bracket in Figure 3B). Although beyond the present scope of this study, the evidence of cell migration in many areas suggests that the QD-CL4-JB577 could be used to study migratory patterns in the developing nervous system and how this could potentially be used to deliver peptides and proteins to all regions of the brain.

Widespread Distribution of QD-CL4-JB577 in the Developing Central Nervous System at E8. We observed maximum brain labeling around E8 at which time QDs were distributed extensively and uniformly throughout the entire brain, forebrain, midbrain, and hindbrain, forming distinct patterns of labeling, as observed from longitudinal sections of the brain (see Figure 4). Although the QDs tend to densely populate some regions over others (especially ventricular areas), confocal microscopy confirmed that QDs generally labeled the entire brain at E8 from forebrain to hindbrain. Also, aggregation of QDs in the ventricular walls was occasionally evident (Figure 4). Confocal microscopy further confirmed that the fluorescent particles detected were not surface artifacts but were inside the cells.[9] This widespread distribution of the QDs was encouraging from the point of view of eventually treating genetic disease where each cell bears the lethal mutation.

As evident from the distribution of the QDs in midbrain at E8, the layer of heavily QD-labeled cells (Figure 4, bracket) most likely corresponds to the neuronal layer which formed from neural stem cells located at the ventricular zone at the time of QD delivery (E4). These observations confirm the significant initial intracellular uptake of QDs at the time of their delivery. Since QDs were evident in the ventricles for a few days after the initial delivery, it is probable that incorporation of QDs into the tissue proceeds for several days. This would also help explain why the QD emission decreases from E8 onward. The extensive labeling by QDs transported along the spinal cord and throughout the developing brain to all types of cells and the developing brain from E6 to E15, and even a small amount of labeling at E19 compares favorably with the localized distribution of viral constructs following injection into brain.[28] While the QDs were numerous and uniform at E8, the continual differentiation of cells and increase in brain size[32] was associated with the formation of complex structures absent from the early developmental stages such as the choroid plexus. These became evident by E11, and became intensely labeled from E11 to E15. After E15, the level of QD labeling declined steeply so that QDs were mostly undetectable at E21.

Changing Pattern of QD Distribution with Developmental Time. In order to track the labeling pattern in brain as development progresses, embryos injected in the spinal canal with QD at E4 were sacrificed at E8, E11, E15, E19, and E21 (hatching) days (3−4 embryos per age) and processed for fluorescent analysis. A representative section from the different developmental ages is depicted in Figure 5 in order to appreciate the overall labeling pattern. A view of a random but representative areas (box) with both DAPI staining (middle panel) and QDs alone (lower panel) showed no abnormalities attributable to the QDs. Although they only represent a small region of the brain, the lower panels are accurate indicators of the frequency of fluorescent QDs (roughly corresponding to the amount of QDs in a given cross-sectional area) at each stage of development. Using ImageJ, Z-stack analysis of E15 brain sections selected at random showed that approximately 50% of detectable QDs were intracellular (inside cells) (data not shown). Comparison of the fluorescence intensities and

DOI: 10.1021/acschemneuro.5b00022
ACS Chem. Neurosci. 2015, 6, 494−504

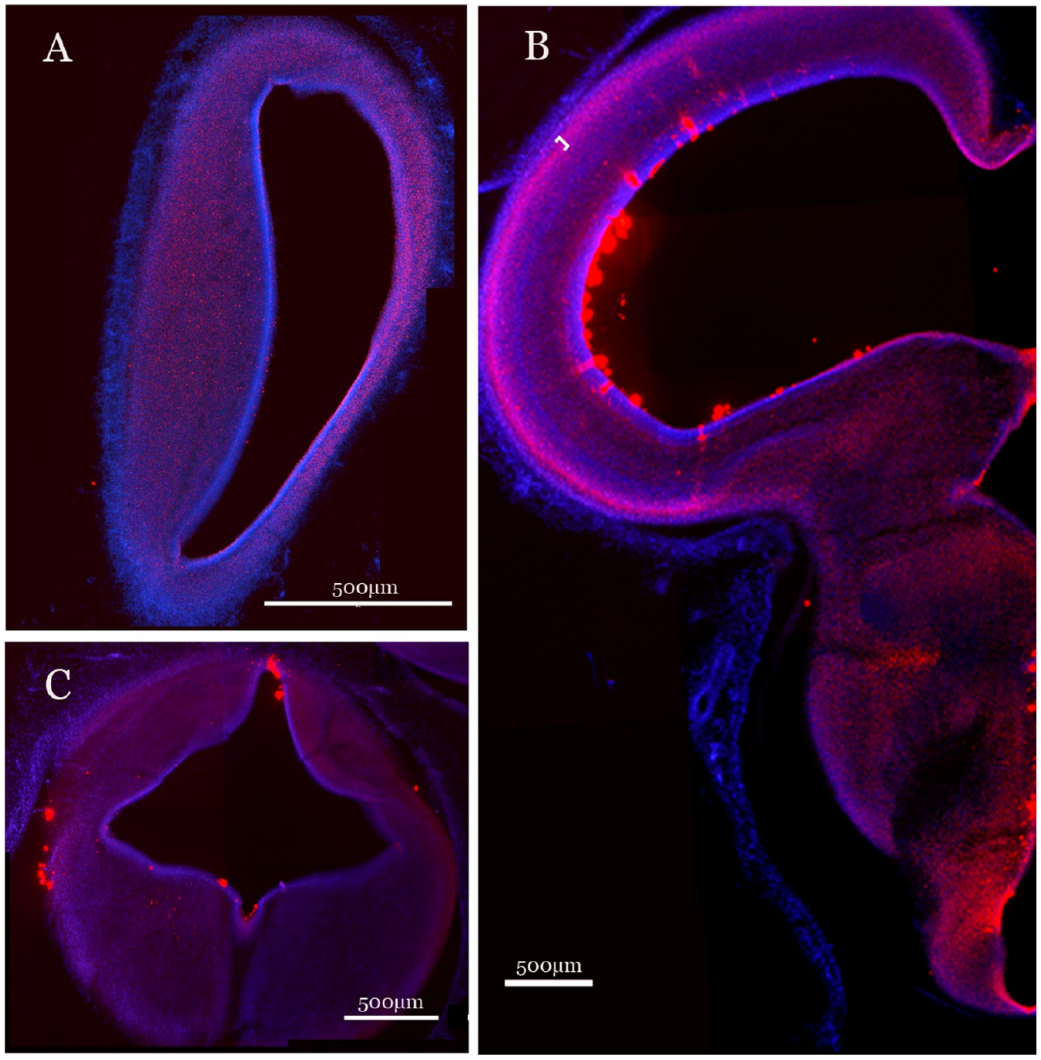

Figure 4. Distribution of QD-peptide conjugates at E8. QD-CL4-JB577 (red) distribution in E8 embryonic chick brain after a spinal canal injection at E4. Representative coronal sections (40 μm) are shown which correspond to forebrain (A), midbrain (B), and hindbrain (C) of the same embryo showing comparable distribution of QDs in the different brain areas at 4 days after injection (E8). A neuronal layer heavily labeled by QDs is indicated by the bracket in B.

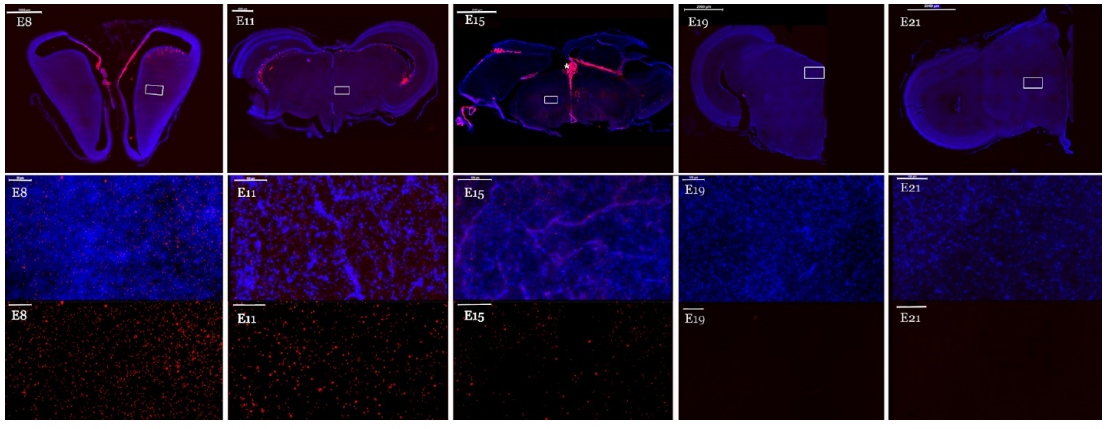

Figure 5. QD-CL4 peptide conjugate distribution at different developmental time points. QD-CL4-JB577 distribution is shown in representative coronal sections of the embryonic chick brain at developmental ages, E8, E11, E15, E19, and E21 from embryos injected at E4. The upper panel shows composites of QD-CL4-JB577 distribution (red fluorescence) in E8 forebrain and E11, E15, E19, and E21 midbrain sections counterstained with DAPI (blue). The middle panel depicts a magnified randomly selected region of each section marked with a white box in each upper panel. The asterisk (*) shows the choroid plexus at E15. The lower panels correspond to each middle panel but only show QD fluorescence. The magnification bar in the upper panel represents 2000 μm and in the middle and bottom panels represents 100 μm.

DOI: 10.1021/acschemneuro.5b00022
ACS Chem. Neurosci. 2015, 6, 494−504

frequencies among each stage of development revealed the following: (i) Peak fluorescence and labeling occurred at E8. (ii) A steep decline in fluorescence and labeling was observed after E15. (iii) Very little fluorescence was detected at E21. Although this was not strictly a quantitative study, we concluded that overall QD labeling was maximum at E8, declined slightly from E8 to E15, and then steeply declined to almost no detectable fluorescence at E21(hatching). Interestingly, some ventricular content can still be observed until E15. Previous studies have shown that the size of the chick brain increases 8-fold from E4 to E6, 10-fold from E6 to E8, and a further 2−3-fold to hatching. Overall, there is a 150-fold increase in size during this time frame so considerable dilution of the dots is expected. However, we believe that some of the dramatic decrease in overall fluorescence is connected to the development of the choroid plexus.

QDs in the Choroid Plexus. At E11, we observed that the labeling pattern dramatically changed (Figure 6A), and that it coincided with the extensive labeling of the choroid plexus (E11, Figure 6B), a structure that develops between E8 and E15 in the chick brain.[33,34] The enrichment of QDs in the choroid plexus was also visible at E15 (Figure 6C). This clearly suggested that the microinjection of QDs had no visible or functional negative impact on the assembly of this complex structure. QDs were injected at E4 when the brain is just a simple neuroepithelium that contains only neural stem cells which are differentiating into neurons. As development progresses, the neural stem cells give rise to astrocyte and oligodendrocyte precursors and eventually to specialized glial cells such as ependymal cells. After migration and terminal differentiation the cells ultimately organize into collective systems with distinct structures and functions. The choroid plexus (CP) is one such structure that can be distinguished from E11 onward and from this study seems to play an important role in the later distribution of QDs. Thus, it was surprising that despite the >100-fold increase in tissue size from E6 to E15, in all experiments we still observed intense staining of the choroid plexus at E15 (Figure 5, upper panel). This intense labeling was transient since it declined rapidly to E18 until it was barely detectable at birth (E21) (Figure 5). The choroid plexus develops on the anterior ventricular roof from a sagitally oriented fold and some posteriorly located transverse folds.[33] It is a collection of modified ependymal cells and capillaries that form a system of producing and distributing cerebrospinal fluid (CSF.) These ependymal cells are glial cells whose apical surface is surrounded by cilia that push around the CSF, similar to the brush-border interface of microvilli in the intestine. Furthermore, they produce CSF and transfer the fluid through tight junctions and so effectively secrete the QDs. By E11, round cells start to appear on the entire plexus (Figure 6A). The QD-CL4-JB577 injected at E4 were stable enough to extensively label the developing choroid plexus 11 days later, and both the E11 and E15 samples clearly showed the expected folds of the CP (see Figure 6B and C). Concurrently, QD labeling was more concentrated in the CP compared to the other regions of the brain. While E8 samples showed uniform distribution of QDs, E11 and E15 samples displayed a shift in fluorescence toward the CP and less fluorescence in other regions. Ultimately, at birth (E21), fluorescence was barely detectable (Figure 5).

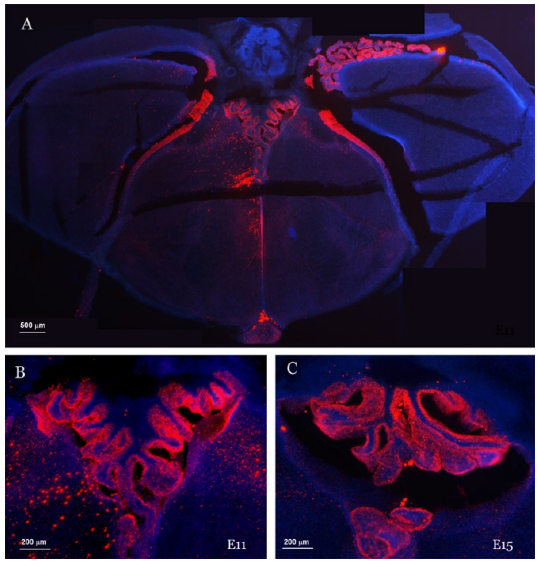

Figure 6. QD-CL4-JB577 conjugate extensively labels cells in the choroid plexus at E11 through E15. (A) Coronal section through the third ventricle showing the labeling pattern at E11. (B) Higher magnified view of the developing choroid plexus at E11. (C) Higher magnified view of the developing choroid plexus at E15. The choroid plexus has not developed at E4 when the QD-CL4-JB577 is microinjected.

Neural Differentiation after QD Incorporation. Since the QD were injected in a critical period of neural differentiation and expansion of neural precursors, it was important to verify that the progression into different neural cell types was not affected by their presence or incorporation. To this end we compared the expression patterns of different known markers of neural stem cells and their differentiated progeny between E8 brains from embryos injected at E4 with either QD-CL4-JB577 or control vehicle (5% DMSO). mRNA in situ hybridization was then used to show that the expression pattern of the transcription factor SOX2, proteolipid protein (PLP), class III-tubulin beta (TUBB3), and brain lipid binding protein (BLBP) was normal in E8 and E15 midbrain and hindbrain (Figure 7). The timing and pattern of expression of these markers is extremely conserved and quickly shifts as the cells differentiate, making them ideal indicators of developmental progression.

SOX2 mRNA is strongly expressed in proliferating neural precursors and differentiation induces downregulation of SOX2, although expression is subsequently transiently upregulated in some subpopulations of mature neurons.[30] At E8 and E15, we detected expression of SOX2 mRNA associated with the ventricular zone precursors (neural stem cells) and a specific layer of mature neurons in the midbrain in sections from both QD and vehicle injected embryos (Figure 7). The absence of any detectable change in the pattern of expression gives further support to the benign nature of the QDs and JB577 used in this study.

Proteolipid protein (PLP) mRNA is expressed in oligodendrocyte progenitors at E8 on cells located in the ventral midline.[35] The expression pattern of PLP was as expected and showed no differences between QD-CL4-JB577 and 5% DMSO- injected embryos. Additionally, the PLP expression pattern was also analyzed later on in development (E15) during the expansion of oligodendrocyte precursors in chicks with similar patterns of expression noted for both QD and 5% DMSO-injected brains (Figure 7), further suggesting the lack of overt or gross toxicity originating from the QDs used in this

DOI: 10.1021/acschemneuro.5b00022
ACS Chem. Neurosci. 2015, 6, 494−504

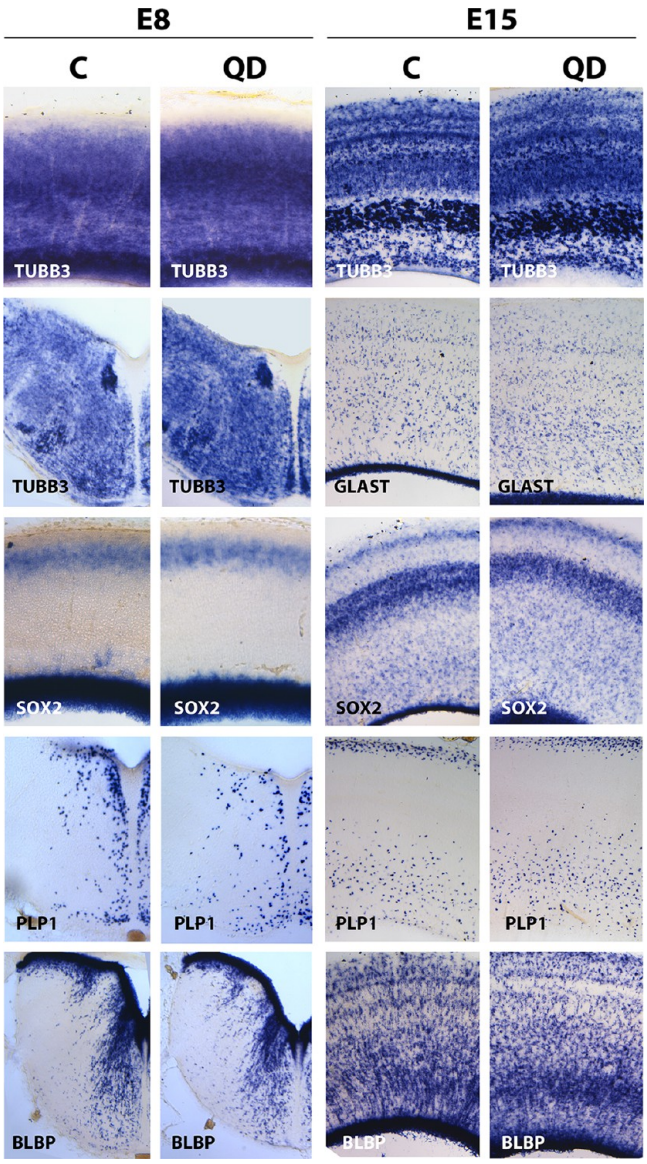

Figure 7. QD-CL4-JB577 does not affect the expression of key transcription factors and cell markers during embryonic development. Brains from embryos injected at E4 with QD-CL4-JB577 conjugates (QD) or 5% DMSO/dye control (C) were collected at E8 and E15 and processed for mRNA in situ hybridization as described in the Methods. Sections from hindbrain and optic tectum were hybridized with sense RNA probes for the markers TUBB3 (class III-β-tubulin), PLP (proteolipid protein), BLBP (brain lipid-binding protein), GLAST (solute carrier family 1 (glial high affinity glutamate transporter) member 3), and the transcription factor SOX2. Results are representative of 3 independent experiments involving 18 control and 18 QD-injected embryos. Comparable levels and distribution of transcripts for all these genes were observed between the two groups indicating that QD-CL4-JB577 conjugates injected at E4 did not alter the migration, proliferation, and survival of developing neurons (TUBB3), oligodendrocytes (PLP), astrocyte precursors (GLAST, BLBP), and neural stem cells (SOX2) at E8 or E15.

study. We chose to compare the expression of the brain-specific member of the lipid-binding protein family (BLBP) since its expression is spatially and temporally correlated with neural differentiation in many parts of the CNS, including in the postnatal cerebellum, embryonic spinal cord, and cerebral cortex. BLBP is transiently expressed in radial glia in the embryonic ventricular zone[36] and it is required for the establishment of the radial glial fiber system necessary for the migration of immature neurons to establish cortical layers.[37] Thus, our finding that expression of BLBP is normal in E8 hindbrain radial glial is strong evidence that chick brain development was unaffected by QD injection. After neuronal migration, the BLBP positive precursors migrate away from the ventricle and initiate the astrocytic phase of the differentiation process. By E15, this process is well underway in the chick midbrain and expression of BLBP in QDs and vehicle injected brain was the same (Figure 7). We also analyzed the expression of GLAST (solute carrier family 1 (glial high affinity glutamate transporter) member 3) at E15. GLAST belongs to an astroglial glutamate transporter family which maintain physiological extracellular glutamate concentrations and are expressed by astrocyte precursors.[38,39] Their expression correlates with the status of glial differentiation/maturation, making them a good measure of normal brain developmental progress. Again GLAST expression was unaffected by the QDs (Figure 7). Lastly, we present evidence that beta-tubulin-III (TUBB3), which is expressed in postmitotic neurons, was also normally expressed in the midbrain and hindbrain regions at E8 and E15 and was unaffected by QD incorporation (Figure 7). In particular, in E15 midbrain the expected number of neuronal layers along with their distribution and thickness was observed in the QD-injected brain indicating that the neuronal cell proliferation over generations and migration is occurring normally in these brains. We have previously used similar in situ hybridization assays to demonstrate increases in expression of astrocyte differentiation genes GFAP (glial fibrillary acidic protein), GLAST, and GS (glutamine synthase) in the nanomelic chick which lacks aggrecan (a proteoglycan with a major role in glial cell maturation) and in chick injury models.[18,35] Thus, the absence of any change in this expression is good evidence of lack of toxicity of the QDs and the chicks appeared normal at hatching.

There have been many attempts to deliver QDs to cells and tissues by either passive delivery, relying on surface functionalization and charge,[6−8] active delivery, such as electroporation, or facilitated delivery, where, for example, a cell-penetrating peptide and the cargo are conjugated to the QD.[9,40,41] However, relatively few studies have followed the fate of QDs in a living, intact brain.[15,42] We therefore designed a novel microinjection system to deliver a precise amount of the synthetic lipopeptide JB577[6−8] into the spinal cord of a developing chick embryo at E4 and showed that the QD-complex was initially targeted to neurostem cells and the neuroblasts present in the brain at time of the injection. Distribution was even and widespread, with very little sign of QD aggregation or chemical instability in tissues. Because of the high intrinsic fluorescence of the QDs used, we were able to follow the fate of the QDs in the chick brain through hatching (17 days later at E21), even though its volume increased >150-fold.[32]

Successful microinjection of QDs at E4 resulted in extensive labeling at E6, and replacing the choice of a neutral PEG coating with a zwitterionic compact ligand, "CL4" (Figure 1) gave improved distribution of label at both E6 and E8. Therefore, for all the subsequent studies described, we used QDs coated with CL4 to which JB577 was attached via the His6-linkage. The uniform labeling of QDs along the spinal tract not only demonstrates the broad perfusion of QDs into the administered region but also the ability of the QDs to

DOI: 10.1021/acschemneuro.5b00022
ACS Chem. Neurosci. 2015, 6, 494−504

migrate a significant distance from the site of injection along the spinal cord canal and into the ventricular system of the brain, penetrating the surrounding nervous system tissue in the process. Whereas our previous study explored the cell-type specific targeting of different types of QDs in specified cell types,[9] the present study explored the widespread-distribution of QDs in the central nervous system in a model system as it developed. At the time of delivery of the QD (E4), the neural plate has already closed, a neural tube has formed along the whole longitudinal axis of the embryo, and the neuroepithelium cells have gone through several cell divisions. At this stage, most of the cells are migrating neuroblasts or neural stem cells of radial glial morphology, which remain associated with the ventricular zone.[17,19,28,31] We conclude that significant amounts of QDs are taken up by these cells and then distributed to their progeny as they migrate radially, carrying their QDs with them.

Evidence that normal milestones were achieved in E8- and E15-brains which received QDs was provided by a series of in situ hybridization studies. TUBB3 expression was high and well-distributed in the expected patterns, indicating normal generation and migration of neurons. The transcription factor SOX-2[29,30] showed a normal pattern of expression as well indicating that neural stem cells distribution and survival were unaffected by the QDs. Glial cell markers PLP, BLBP, and GLAST[18,35−38] appeared at the expected time and in normal distribution patterns, suggesting that developmental progression to the gliogenic phase of brain development was proceeding normally. We conclude that there was no evidence of growth retardation or acceleration of growth or differentiation. The chickens developed normally and hatched from their eggs on schedule where they displayed normal pecking and feeding behavior identical to control animals.

We have previously demonstrated that QD-CL4-JB577 particles target the perinuclear region of neuronal cell bodies in the CA3 cell layer of hippocampal slice cultures with no toxicity or morphological changes (up to 72 h in culture). A similar lack of any overt toxicity was observed in the developing chick brain with the same QDs. Both stability and toxicity of the QDs had been an issue in previous studies in which QDs/nanoparticles were administered intravenously in monkeys and mice and in both instances there was diminished overall fluorescence in the long term in in vivo systems.[13,27] We similarly observed a time-dependent decrease in overall fluorescence in our study which greatly accelerated after E11. At E19, only a few QDs were visible in the brain and were scattered throughout the section in a seemingly sporadic rather than the uniform manner observed at E8-E15. However, the structure of the brain appeared completely normal. Between E15 and E19, the choroid plexus was no longer intensely labeled by QDs, and overall fluorescence was greatly reduced. The QDs were most likely transported out of the brain after the embryo developed its functioning choroid plexus. The structure likely recognized the QD/CL4s/QD-CL4-JB577 as foreign particles, and removed QDs from circulation in the brain. Previous studies[22] suggest stability in vivo up to 90 days so they are unlikely to have ceased to be emissive due to formation of surface defects or traps or to be degraded sufficiently to release Cd^{2+} ions to the intracellular and intercellular environments. One additional factor is that a significant dilution of the QDs occurs because the brain increases in volume some 150-fold and after the development of the choroid plexus there is accelerated removal of QDs via the glymphatic system.[43] We conclude that a combination of these explanations is the most likely.

The main advantage of chemically synthesizing QDs with negatively charged coats (CL4) and a cell-penetrating peptide (JB577) is that they can deliver additional cargo beyond the 25 peptides/QD. Should the Cd prove to be toxic in future studies, we can replace them with less toxic QD materials such as those with InP cores.[7,10,11] Interestingly, reports focusing on the toxicity issue are somewhat inconsistent in terms of answering major issues. Mice injected with amphiphilic PEG-coated QDs at 20 pmol/g animal weight were viable until necropsy at 133 days. However, injection of maltodextrin coated CdSe QDs into the air sac of early stage E1−2 chickens was reported to be extremely cytotoxic and embryotoxic.[44] We believe this difference from our experience with embryonic chicks to be primarily a technical issue, either the quality of the nanoparticles or the time of injection (E1−2 compared with E4 in our study) or the use of airsac absorption. There was certainly no indication of any intrinsic toxicity of QDs as we prepare them. Moreover, we note that the Cd in those core-only QDs had direct access to the biological environment and were not protected by an overcoating shell as our materials are. Another report of toxicity occurred when a synthetic peptide (APWH-LSSQYSRT) was conjugated to CdSe/ZnS QDs and targeted to Rhesus monkey embryonic stem cells. This study used a small S-CH_2COOH QD coating, which is known to undergo pH dependent aggregation,[7] something that is not an issue for the DHLA-based zwitterionic coatings used in this and our previous studies.[21] More in agreement with our findings is a recent long-term study in Rhesus monkeys which showed the QDs to be intact in the body for up to 90 days and showing no toxicity after 3 years.[27]

The primary aim of this study was to show that we could deliver a QD-peptide functionalized construct to an intact normally developing nervous system and observe the distribution of the QDs with their surface cargo to all brain regions. This has been achieved, and we have supplied ample evidence that our QD constructs produced minimal observable gross or overt toxicity in chicken embryos. We suggest that the previously observed QD toxicity is very much dependent on the conditions of their use, the composition of the QD core and whether it is protected by an overcoating layer, the chemicals used to coat the QDs, the conjugated peptides attached to the QDs, and the technique used to administer the QDs. We conclude that, by carefully choosing the chemistry of the core and coating, QDs have the potential to be safe for long-term research applications such as demonstrating that JB577 can function as a chemical chaperone in the CNS.

A major barrier to applying chemistry to treating neurodegenerative disease with QDs is the blood-brain barrier. This study does not address this question directly since we injected directly into the spinal cord, but we believe that the uniform distribution of the QD label in the brain suggests that JB577 is functioning as a brain barrier cell-penetrating peptide. Previously, nanoparticle (NP) iron chelators have been used with limited success to treat Alzheimer's disease and other neurologic disorders while PEGylated polymeric NPs have been tried therapeutically in prion diseases but with limited success.[45] Other strategies to target the brain with NPs have taken advantage of the interaction with specific receptor-mediated transport such as the transferrin receptor (TFR). TFR binding antibodies were attached to cell penetrating peptides, and melanotransferrin was incorporated into chimeric constructs but all have met with limited success. Polysorbate 8038 and antitransferrin receptor monoclonal antibodies

DOI: 10.1021/acschemneuro.5b00022
ACS Chem. Neurosci. 2015, 6, 494−504

(MAbs) have been tested extensively but a lot of research is still needed before they can be considered for treatment of human diseases. The hexapeptide dalargin, tubocurarine, and the lipid-soluble P-glycoprotein substrates loperamide-45 and doxorubicin have all been coupled to polysorbate 80-coated nanoparticles to little avail,[46] so we conclude that QDs with the appropriate chemical modifications (QD-CL4-JB577) have enormous potential to overcome the failures of traditional therapeutics, which often fail because of poor water solubility or a lack of target specificity.[42,46]

In summary, we conclude that QDs offer the exciting potential of uniformly delivering small molecule therapeutics or peptides (or proteins) to the developing brain in a model system together with the equally important ability to directly track chemically synthesized, biologically active compounds and see if they are actually delivered to the correct cells and subcellular compartments. This is especially critical if, for example, QDs were to be used to deliver pharmacological chaperones to promote folding of misfolded proteins in the ER[47−49] in inherited diseases resulting from a single missense mutation in a gene. In our example, the drug is a small molecule inhibitor of the enzyme palmitoyl:protein thioesterase[48,49] (the DAP1 structure incorporated into JB577) which functions as a chaperone. By coupling to QDs, we can follow its fate in detail. To date, there is only one chemical chaperone (Migalastat) which is believed to function as a chaperone in certain patients with α-galactosidase deficiency (Fabry disease),[47] but this is clearly a rapidly expanding area of small molecule chemical therapeutics in the CNS with great potential to benefit from the unique properties that nanoparticles such as QDs can provide.

METHODS

Quantum Dots. CdSe/ZnS core/shell QDs[50] with an emission maxima centered at 625 nm were from Invitrogen Life Technologies (Carlsbad, CA) and were made hydrophilic by exchanging the native surface with DHLA (dihydrolipoic acid) appended to either polyethylene glycol (PEG, Mw ∼ 750/∼15 ethylene oxide repeats) terminating in a methoxy group or the zwitterionic compact ligand CL4 as described previously.[21,22] These are referred to as DHLA-PEG or DHLA-CL4 ligands/QDs.

Peptides. The palmitoylated peptide (JB577, WGDap(Palmitoyl)-VKIKKP9GGH6, N-terminal acetylated/C-terminal amidated) sequence used was based on that of Ras-4A(GC(Palmitoyl) VKIKK)[51] where "Palmitoyl" corresponds to a C16:0 palmitate group that is covalently attached to a nonhydrolyzable diaminopropionic acid (Dap) functionality synthesized into the peptide backbone. All peptides were synthesized using Boc-solid phase peptide synthesis,[6,8,52] purified by HPLC, and characterized by electrospray ionization mass spectrometry. All peptide sequences are written in the conventional amino-to-carboxy terminus orientation.

Quantum Dot-Peptide Bioconjugate Microinjection into the Embryonic Spinal Cord. QD-Palm-1 bioconjugates were diluted from a stock solution of preformed peptide-QD complexes (1 μM QD assembled with a ratio of 25 JB577 peptides per QD-CL4 in 5% DMSO in PBS) into complete growth medium to a final QD concentration of 50−100 nM for 1 h. Fertilized White Leghorn chicken (*Gallus gallus*) eggs were obtained from Sunnyside Hatchery (Beaver Dam, WI) and incubated at 37.9 °C and 90% relative humidity in a Midwest incubator. At embryonic day 4 (E4) (stage 21), chicken embryos were made directly accessible by cutting a window in the eggshell and carefully removing the extra-embryonic membranes covering the embryo, using forceps and spring scissors. Injection of a mixture of QD-CL4/PEG-JB577 and methyl green (0.25 mg/mL) into the central canal of the spinal cord was performed with a glass capillary needle. Control embryos were injected with vehicle solution (5% DMSO, 0.25 mg/mL methyl green in PBS). The maximum injection volume (2−4 μL) was achieved when the dye injected into the ventricle by this new procedure had reached the brain vesicle as visualized by the distribution of the methyl green colored solution. After retraction of the capillary, the embryo was hydrated with sterile PBS, the window in the eggshell was resealed with 3 M vinyl tape, and the embryos allowed to incubate for the specified times.[18] As with all similar studies, including those designed to electroporate DNA constructs at E4,[53,54] there was an average of 50% mortality in injected chick embryos from damaging the allantoic and vitelline extra-embryonic vessels during the procedure. Typically we injected 18 embryos with QD-peptide conjugates and dye and compared this to 18 injected with dye alone over the time period studied. There was no difference in mortality between QD-injected and control animals. A total of 180 eggs over a period of 2 years were microinjected for these studies. We observed no size or gross physical differences between control and QD-injected chick embryos during these experiments. All age embryos were euthanized by decapitation prior to dissection of the brain in agreement with recommendations of the Institute for Laboratory Animal Research, the NIH intramural recommendations for rodent neonates, and the AVMA Panel on Euthanasia.

Histology. Eggs were removed from the incubator after their allotted incubation period (E6, E8, E11, E15, E19, E21), embryos harvested, and the brains dissected and fixed in 4% paraformaldehyde in PBS (PFA).[25−27] E11 embryos and older were euthanized by decapitation prior to dissection of the brain in agreement with recommendations of ILAR, the NIH intramural recommendations for rodent neonates, and the AVMA Panel on Euthanasia. Brains and spinal cords dissected from fixed bodies or heads were cryoprotected by incubation in 20% sucrose, 10% formalin in PBS solution for 24 h, embedded in 10% gelatin, 20% sucrose blocks and cut into 40 μm sections using a SM 2000R Leica microtome. Sections were mounted on Superfrost Plus glass slides (Fisherbrand, Pittsburgh,PA). Nuclei were counterstained with DAPI.

mRNA in Situ Hybridization. To prepare the digoxigenin (DIG)-labeled RNA probes used for in situ hybridizations, cDNA fragments from the PLP (proteolipid protein), TUBB3 (class III-β-tubulin), and BLBP (brain lipid binding protein) genes were prepared as previously described.[18,35] cDNA fragments for SOX2 (SRY-related HMG-box gene 2) (nucleotides 402−948 of GenBank: D50603.1) was obtained by PCR from E8 chick brain cDNA using specific primers based on GenBank sequences. Riboprobes incorporating DIG-labeled nucleotides were synthesized from linearized plasmid templates with SP6 or T7 polymerase (Roche). Slices of 40 μm were prepared for mRNA in situ hybridization as described previously.[18,35,55] After hybridization, DIG-labeled RNA duplexes were detected with an alkaline phosphatase-conjugated anti-DIG antibody (Roche). Alkaline phosphatase activity was then detected using 5-bromo-4-chloro-3′-indolyphosphate *p*-toluidine (BCIP) and nitro-blue tetrazolium (NBT) substrates (Roche) as described previously.[18,35,55]

Microscopy and Image Analysis. The intracellular distribution of QDs was assessed from fluorescent images obtained with a Leica SP2 spectral confocal microscope in the Integrated Light Microscopy Core Facility of The University of Chicago Cancer Research Center. Complete brain images were reconstructed as montages from individual images (obtained with a Zeiss AxioCam Mrtm) through manual tiling (<20 images) or automatic tiling (20−100 images). ImageJ software was used for image analysis.

Simulating the QD Ligand and Peptide Structures. The hard core−shell structure of the 625 nm emitting QD is a sphere of diameter ∼10 nm based on TEM analysis. The DHLA-PEG ligand is a shell extending ∼30 Å from the QD surface, and the DHLA-CL4 ligand is a shell extending 16.2 Å from the QD surface. The DHLA-CL4 extension used is based on previous results along with energy minimization[21] and suggests that the ligand only extends to the portion of the peptide corresponding to the Gly2-Pro9 interface. It is important to note that these ligands may actually be even more compacted than depicted here (Figure 1). The palmitoylated peptide (JB577) is shown as a ball and stick structure oriented onto the QD surface by the terminal hexahistidine (His_6) motif. These structural models were created using the same methods as described previously[8]

DOI: 10.1021/acschemneuro.5b00022
ACS Chem. Neurosci. 2015, 6, 494−504

and only suggest one of many different possible configurations for each.

AUTHOR INFORMATION

Corresponding Author

*Mailing address: 5841 S. Maryland Ave., MC5058, Chicago, IL 60637. E-mail: dawg@uchicago.edu.

Author Contributions

R.A., under the direction of M.S.D. carried out the experiments on the chicks, performed the microscopy, analyzed the data, and both R.A. and M.S.D. helped write the manuscript. M.S.D. also did the injections and supervised J.H. in the preparation of brain slices. N.B.S. was in overall charge of the chick project (financing, eggs, space, equipment, etc.) and had editorial contributions to the writing of the manuscript. I.M. and J.B.D. had oversight of the chemistry and cell biology of the project and made editorial contributions. M.H.S., K.S., and A.L.H. were involved in the synthesis of the quantum dots and the chemistry of the coating. P.E.D. conceived, directed, and funded the synthesis of the peptide JB577 by V.P.. He has been involved with the chemical chaperone concept for many years. G.D. conceived the project, arranged to collaborate with I.M., J.B.D., and P.E.D., wrote the manuscript, and bears ultimate responsibility for the quality of the work presented.

Funding

This work was supported by USPHS [Grant number NS36866-38 (to G.D.)] and P50 Grant [Grant Number HD09402 (to G.D. N.B.S., and M.S.D.)], as well as the Children Brain Disease Foundation to G.D. I.M. and A.L.H. were supported by NRL, the NRL NSI, ONR, DARPA and DTRA JSTO [MIPR B112582M]. P.E.D. was supported by GM-098871 from the USPHS, and V.P. acknowledges the Ramón Areces foundation for financial support.

Notes

The authors declare no competing financial interest.

ACKNOWLEDGMENTS

We thank Vitas Bindokas and Christine Labno in the Integrated Light Microscopy Core Facility of The University of Chicago Cancer Research Center for help and advice with the interpretation of images.

ABBREVIATIONS

QDs, quantum dots; E, embryonic day; PEG, polyethylene glycol; CL4, compact ligand 4 (zwitterionic); JB577, WGDap-(Palmitoyl)VKIKKP9GGH6

REFERENCES

(1) Ravenstijn, P. G., Drenth, H. J., O'Neill, M. J., Danhof, M., and de Lange, E. C. (2012) Evaluation of blood-brain barrier transport and CNS drug metabolism in diseased and control brain after intravenous L-DOPA in a unilateral rat model of Parkinson's disease. *Fluids Barriers CNS 9*, 4.

(2) Son, S., Hwang, D. W., Singha, K., Jeong, J. H., Park, T. G., Lee, D. S., and Kim, W. J. (2011) RVG peptide tethered bioreducible polyethylenimine for gene delivery to brain. *J. Controlled Release 155*, 18−25.

(3) Alvarez-Erviti, L., Seow, Y., Yin, H., Betts, C., Lakhal, S., and Wood, M. J. (2011) Delivery of siRNA to the mouse brain by systemic injection of targeted exosomes. *Nat. Biotechnol. 29*, 341−345.

(4) Sharma, G., Modgil, A., Zhong, T., Sun, C., and Singh, J. (2014) Influence of short-chain cell-penetrating peptides on transport of Doxorubicin encapsulating receptor-targeted liposomes across brain endothelial barrier. *Pharm. Res. 31*, 1194−1209.

(5) Cooper, I., Sasson, K., Teichberg, V. I., Schnaider-Beeri, M., Fridkin, M., and Shechter, Y. (2012) Peptide derived from HIV-1 TAT protein destabilizes a monolayer of endothelial cells in an in vitro model of the blood-brain barrier and allows permeation of high molecular weight proteins. *J. Biol. Chem. 287*, 44676−44683.

(6) Delehanty, J. B., Bradburne, C. E., Boeneman, K., Susumu, K., Farrell, D., Mei, B. C., Blanco-Canosa, J. B., Dawson, G., Dawson, P. E., Mattoussi, H., and Medintz, I. L. (2010) Delivering quantum dot-peptide bioconjugates to the cellular cytosol: escaping from the endolysosomal system. *Integr Biol. 2*, 265−277.

(7) Algar, W. R., Susumu, K., Delehanty, J. B., and Medintz, I. L. (2011) Semiconductor quantum dots in bioanalysis: crossing the valley of death. *Anal. Chem. 83*, 8826−8837.

(8) Boeneman, K., Delehanty, J. B., Blanco-Canosa, J. B., Susumu, K., Stewart, M. H., Oh, E., Huston, A. L., Dawson, G., Ingale, S., Walters, R., Domowicz, M., Deschamps, J. R., Algar, W. R., Dimaggio, S., Manono, J., Spillmann, C. M., Thompson, D., Jennings, T. L., Dawson, P. E., and Medintz, I. L. (2013) Selecting improved peptidyl motifs for cytosolic delivery of disparate protein and nanoparticle materials. *ACS Nano 7*, 3778−3796.

(9) Walters, R., Kraig, R. P., Medintz, I., Delehanty, J. B., Stewart, M. H., Susumu, K., Huston, A. L., Dawson, P. E., and Dawson, G. (2012) Nanoparticle targeting to neurons in a rat hippocampal slice culture model. *ASN Neuro 4*, 383−392.

(10) Delehanty, J. B., Boeneman, K., Bradburne, C. E., Robertson, K., and Medintz, I. L. (2009) Quantum dots: a powerful tool for understanding the intricacies of nanoparticle-mediated drug delivery. *Expert Opin. Drug Delivery 6*, 1091−1112.

(11) Petryayeva, E., Algar, W. R., and Medintz, I. L. (2013) Quantum dots in bioanalysis: a review of applications across various platforms for fluorescence spectroscopy and imaging. *Appl. Spectrosc. 67*, 215−252.

(12) Rehberg, M., Praetner, M., Leite, C. F., Reichel, C. A., Bihari, P., Mildner, K., Duhr, S., Zeuschner, D., and Krombach, F. (2010) Quantum dots modulate leukocyte adhesion and transmigration depending on their surface modification. *Nano Lett. 10*, 3656−3664.

(13) Cai, W., Shin, D. W., Chen, K., Gheysens, O., Cao, Q., Wang, S. X., Gambhir, S. S., and Chen, X. (2006) Peptide-labeled near-infrared quantum dots for imaging tumor vasculature in living subjects. *Nano Lett. 6*, 669−676.

(14) Minami, S. S., Sun, B., Popat, K., Kauppinen, T., Pleiss, M., Zhou, Y., Ward, M. E., Floreancig, P., Mucke, L., Desai, T., and Gan, L. (2012) Selective targeting of microglia by quantum dots. *J. Neuroinflammation 9*, 22.

(15) Jung, J., Solanki, A., Memoli, K. A., Kamei, K., Kim, H., Drahl, M. A., Williams, L. J., Tseng, H. R., and Lee, K. (2010) Selective inhibition of human brain tumor cells through multifunctional quantum-dot-based siRNA delivery. *Angew. Chem., Int. Ed. 49*, 103−107.

(16) Haydar, T. F., Bambrick, L. L., Krueger, B. K., and Rakic, P. (1999) Organotypic slice cultures for analysis of proliferation, cell death, and migration in the embryonic neocortex. *Brain Res. Brain Res. Protoc. 4*, 425−437.

(17) Kakita, A., and Goldman, J. E. (1999) Patterns and dynamics of SVZ cell migration in the postnatal forebrain: Monitoring living progenitors in slice preparations. *Neuron 23*, 461−472.

(18) Domowicz, M. S., Henry, J. G., Wadlington, N., Navarro, A., Kraig, R. P., and Schwartz, N. B. (2011) Astrocyte precursor response to embryonic brain injury. *Brain Res. 1389*, 35−49.

(19) Gray, G. E., and Sanes, J. R. (1991) Migratory paths and phenotypic choices of clonally related cells in the avian optic tectum. *Neuron 6*, 211−225.

(20) LaVail, J. H., and Cowan, W. M. (1971) The development of the chick optic tectum. I. Normal morphology and cytoarchitectonic development. *Brain Res. 28*, 391−419.

(21) Susumu, K., Oh, E., Delehanty, J. B., Blanco-Canosa, J. B., Johnson, B. J., Jain, V., Hervey, W. J. t., Algar, W. R., Boeneman, K.,

DOI: 10.1021/acschemneuro.5b00022
ACS Chem. Neurosci. 2015, 6, 494−504

Dawson, P. E., and Medintz, I. L. (2011) Multifunctional compact zwitterionic ligands for preparing robust biocompatible semiconductor quantum dots and gold nanoparticles. *J. Am. Chem. Soc. 133*, 9480−9496.
(22) Mei, B. C., Susumu, K., Medintz, I. L., Delehanty, J. B., Mountziaris, T. J., and Mattoussi, H. (2008) Modular poly(ethylene glycol) ligands for biocompatible semiconductor and gold nanocrystals with extended pH and ionic stability. *J. Mater. Chem. 18*, 4949−4958.
(23) Prasuhn, D. E., Deschamps, J. R., Susumu, K., Stewart, M. H., Boeneman, K., Blanco-Canosa, J. B., Dawson, P. E., and Medintz, I. L. (2010) Polyvalent display and packing of peptides and proteins on semiconductor quantum dots: Predicted versus experimental results. *Small 6*, 555−564.
(24) Blanco-Canosa, J. B., Wu, M., Susumu, K., Petryayeva, E., Jennings, T. L., Dawson, P. E., Algar, W. R., and Medintz, I. L. (2014) Recent progress in the bioconjugation of quantum dots. *Coord. Chem. Rev. 263*, 101−137.
(25) Zhan, N., Palui, G., Safi, M., Ji, X., and Mattoussi, H. (2013) Multidentate zwitterionic ligands provide compact and highly biocompatible quantum dots. *J. Am. Chem. Soc. 135*, 13786−13795.
(26) Muro, E., Fragola, A., Pons, T., Lequeux, N., Ioannou, A., Skourides, P., and Dubertret, B. (2012) Comparing intracellular stability and targeting of sulfobetaine quantum dots with other surface chemistries in live cells. *Small 8*, 1029−1037.
(27) Ye, L., Yong, K. T., Liu, L., Roy, I., Hu, R., Zhu, J., Cai, H., Law, W. C., Liu, J., Wang, K., Liu, J., Liu, Y., Hu, Y., Zhang, X., Swihart, M. T., and Prasad, P. N. (2012) A pilot study in non-human primates shows no adverse response to intravenous injection of quantum dots. *Nat. Nanotechnol. 7*, 453−458.
(28) Cepko, C. L., Golden, J. A., Szele, F. G., and Lin, J. C. (1997) Lineage analysis in the vertebrate central nervous system. In *Molecular and Cellular Approches to Neural Development* (Cowan, W. M., Jessell, T. M., and Zipursky, S. L., Eds.), pp 391−439, Oxford University Press, New York.
(29) Ferri, A. L., Cavallaro, M., Braida, D., Di Cristofano, A., Canta, A., Vezzani, A., Ottolenghi, S., Pandolfi, P. P., Sala, M., DeBiasi, S., and Nicolis, S. K. (2004) Sox2 deficiency causes neurodegeneration and impaired neurogenesis in the adult mouse brain. *Development 131*, 3805−3819.
(30) Uwanogho, D., Rex, M., Cartwright, E. J., Pearl, G., Healy, C., Scotting, P. J., and Sharpe, P. T. (1995) Embryonic expression of the chicken Sox2, Sox3 and Sox11 genes suggests an interactive role in neuronal development. *Mech. Dev. 49*, 23−36.
(31) Alvarez-Buylla, A., Garcia-Verdugo, J. M., and Tramontin, A. D. (2001) A unified hypothesis on the lineage of neural stem cells. *Nat. Rev.. Neurosci. 2*, 287−293.
(32) Charvet, C. J., and Striedter, G. F. (2010) Bigger brains cycle faster before neurogenesis begins: a comparison of brain development between chickens and bobwhite quail. *Proc. Biol. Sci. 277*, 3469−3475.
(33) Dziegielewska, K. M., Ek, J., Habgood, M. D., and Saunders, N. R. (2001) Development of the choroid plexus. *Microsc. Res. Tech. 52*, 5−20.
(34) Kaluza, J. S., Burstone, M. S., and Klatzo, I. (1964) Enzyme histochemistry of the chick choroid plexus. *Acta Neuropathol. 3*, 480−489.
(35) Domowicz, M. S., Sanders, T. A., Ragsdale, C. W., and Schwartz, N. B. (2008) Aggrecan is expressed by embryonic brain glia and regulates astrocyte development. *Dev. Biol. 315*, 114−124.
(36) Kurtz, A., Zimmer, A., Schnutgen, F., Bruning, G., Spener, F., and Muller, T. (1994) The expression pattern of a novel gene encoding brain-fatty acid binding protein correlates with neuronal and glial cell development. *Development 120*, 2637−2649.
(37) Feng, L., Hatten, M. E., and Heintz, N. (1994) Brain lipid-binding protein (BLBP): A novel signaling system in the developing mammalian CNS. *Neuron 12*, 895−908.
(38) Shibata, T., Yamada, K., Watanabe, M., Ikenaka, K., Wada, K., Tanaka, K., and Inoue, Y. (1997) Glutamate transporter GLAST is expressed in the radial glia-astrocyte lineage of developing mouse spinal cord. *J. Neurosci. 17*, 9212−9219.
(39) Deneen, B., Ho, R., Lukaszewicz, A., Hochstim, C. J., Gronostajski, R. M., and Anderson, D. J. (2006) The transcription factor NFIA controls the onset of gliogenesis in the developing spinal cord. *Neuron 52*, 953−968.
(40) Smith, B. R., Cheng, Z., De, A., Koh, A. L., Sinclair, R., and Gambhir, S. S. (2008) Real-time intravital imaging of RGD-quantum dot binding to luminal endothelium in mouse tumor neovasculature. *Nano Lett. 8*, 2599−2606.
(41) Akerman, M. E., Chan, W. C., Laakkonen, P., Bhatia, S. N., and Ruoslahti, E. (2002) Nanocrystal targeting in vivo. *Proc. Natl. Acad. Sci. U. S. A. 99*, 12617−12621.
(42) Ruan, Y., Yao, L., Zhang, B., Zhang, S., and Guo, J. (2012) Nanoparticle-mediated delivery of neurotoxin-II to the brain with intranasal administration: An effective strategy to improve anti-nociceptive activity of neurotoxin. *Drug Dev. Ind. Pharm. 38*, 123−128.
(43) Iliff, J. J., Wang, M. H., Zeppenfeld, D. M., Venkataraman, A., Plog, B. A., Liao, Y. H., Deane, R., and Nedergaard, M. (2013) Cerebral arterial pulsation drives paravascular csf-interstitial fluid exchange in the murine brain. *J. Neurosci. 33*, 18190−18199.
(44) Rodriguez-Fragoso, P., Reyes-Esparza, J., Leon-Buitimea, A., and Rodriguez-Fragoso, L. (2012) Synthesis, characterization and toxicological evaluation of maltodextrin capped cadmium sulfide nanoparticles in human cell lines and chicken embryos. *J. Nanobiotechnol. 10*, 47.
(45) Sousa, F., Mandal, S., Garrovo, C., Astolfo, A., Bonifacio, A., Latawiec, D., Menk, R. H., Arfelli, F., Huewel, S., Legname, G., Galla, H. J., and Krol, S. (2010) Functionalized gold nanoparticles: A detailed in vivo multimodal microscopic brain distribution study. *Nanoscale 2*, 2826−2834.
(46) Tsoi, K. M., Dai, Q., Alman, B. A., and Chan, W. C. (2013) Are quantum dots toxic? Exploring the discrepancy between cell culture and animal studies. *Acc. Chem. Res. 46*, 662−671.
(47) Parenti, G. (2009) Treating lysosomal storage diseases with pharmacological chaperones: From concept to clinics. *EMBO Mol. Med. 1*, 268−279.
(48) Dawson, G., Schroeder, C., and Dawson, P. E. (2010) Palmitoyl:protein thioesterase (PPT1) inhibitors can act as pharmacological chaperones in infantile Batten disease. *Biochem. Biophys. Res. Commun. 395*, 66−69.
(49) Dawson, G., Dawson, S. A., Marinzi, C., and Dawson, P. E. (2002) Anti-tumor promoting effects of palmitoyl: protein thioesterase inhibitors against a human neurotumor cell line. *Cancer Lett. 187*, 163−168.
(50) Medintz, I. L., Uyeda, H. T., Goldman, E. R., and Mattoussi, H. (2005) Quantum dot bioconjugates for imaging, labelling and sensing. *Nat. Mater. 4*, 435−446.
(51) Cho, S., Dawson, P. E., and Dawson, G. (2000) In vitro depalmitoylation of neurospecific peptides: implication for infantile neuronal ceroid lipofuscinosis. *J. Neurosci. Res. 59*, 32−38.
(52) Blanco-Canosa, J. B., and Dawson, P. E. (2008) An efficient Fmoc-SPPS approach for the generation of thioester peptide precursors for use in native chemical ligation. *Angew. Chem., Int. Ed. 47*, 6851−6855.
(53) King, L. A., Schwartz, N. B., and Domowicz, M. S. (2009) Glial migratory streams in the developing hindbrain: a slice culture approach. *J. Neurosci Methods 177*, 30−43.
(54) Nakamura, H., and Funahashi, J. (2001) Introduction of DNA into chick embryos by in ovo electroporation. *Methods 24*, 43−48.
(55) Domowicz, M. S., Cortes, M., Henry, J. G., and Schwartz, N. B. (2009) Aggrecan modulation of growth plate morphogenesis. *Dev. Biol. 329*, 242−257.

DOI: 10.1021/acschemneuro.5b00022
ACS Chem. Neurosci. 2015, 6, 494−504